Sustainable Cities and Society 77 (2022) 103564

Contents lists available at ScienceDirect

Sustainable Cities and Society

journal homepage: www.elsevier.com/locate/scs

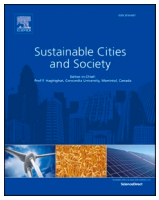

Urban heat island mitigation by green infrastructure in European Functional Urban Areas

Federica Marando [a,*], Mehdi P. Heris [b], Grazia Zulian [a], Angel Udías [a], Lorenzo Mentaschi [c], Nektarios Chrysoulakis [d], David Parastatidis [d], Joachim Maes [a]

[a] European Commission, Joint Research Centre (JRC), Ispra, Italy
[b] Hunter College, Urban Policy & Planning, New York, NY 10065, USA
[c] Department of Physics and Astronomy "Augusto Righi" (DIFA), University of Bologna, Bologna 40127, Italy
[d] Remote Sensing Lab, Institute of Applied and Computational Mathematics, Foundation for Research and Technology Hellas (FORTH), Heraklion 70013, Greece

ARTICLE INFO

Keywords:
Ecosystem services
Urban green infrastructure
Urban heat island
Microclimate regulation
Nature-based solutions

ABSTRACT

The Urban Heat Island (UHI) effect is one of the most harmful environmental hazards for urban dwellers. Climate change is expected to increase the intensity of the UHI effect. In this context, the implementation of Urban Green Infrastructure (UGI) can partially reduce UHI intensity, promoting a resilient urban environment and contributing to climate change adaptation and mitigation. In order to achieve this result, there is a need to systematically integrate UGI into urban planning and legislation, but this process is subject to the availability of widely applicable, easily accessible and quantitative evidence. To offer a big picture of urban heat intensity and opportunities to mitigate high temperatures, we developed a model that reports the Ecosystem Service (ES) of microclimate regulation of UGI in 601 European cities. The model simulates the temperature difference between a baseline and a no-vegetation scenario, extrapolating the role of UGI in mitigating UHI in different urban contexts. Finally, a practical, quantitative indicator that can be applied by policymakers and city administrations has been elaborated, allowing to estimate the amount of urban vegetation that is needed to cool summer temperatures by a certain degree. UGI is found to cool European cities by 1.07 °C on average, and up to 2.9 °C, but in order to achieve a 1 °C drop in urban temperatures, a tree cover of at least 16% is required. The microclimate regulation ES is mostly dependent on the amount of vegetation inside a city and by transpiration and canopy evaporation. Furthermore, in almost 40% of the countries, more than half of the residing population does not benefit from the microclimate regulation service provided by urban vegetation. Widespread implementation of UGI, in particular in arid regions and cities with insufficient tree cover, is key to ensure healthy urban living conditions for citizens.

1. Introduction

The Urban Heat Island (UHI) effect can be described as a distinct urban climate, characterized by higher temperatures in densely built-up areas compared to the surrounding areas (Oke, 1982). This phenomenon is caused by the anthropogenic alteration of the natural environment, such as development of buildings and impervious surfaces. These changes determine a higher heat capacity which traps more energy and radiation with consequent increase in temperature. Urban morphology can also have an influence, increasing the multiple catering of shortwave radiation and trapping the long wave radiation, resulting in an intensification of the heat storage in the city. Additionally, anthropogenic activities, such as heating and transportation further increase the amount of heat released in urban areas, compared to the natural landscape (Zhou, Rybski & Kropp, 2017). The extent and distribution of UHI can be estimated both through air temperature and through Land Surface Temperature (LST) data. The first approach measures, usually with meteorological monitoring stations, the temperature from the ground up to tree height, the "canopy layer" (Schwarz, Schlink, Franck & Großmann, 2012). The second approach measures the temperature of

* Corresponding author.
E-mail addresses: federica.marando@ec.europa.eu (F. Marando), mehdi.heris@hunter.cuny.edu (M.P. Heris), grazia.zulian@ec.europa.eu (G. Zulian), angel.udias-moinelo@ec.europa.eu (A. Udías), lorenzo.mentaschi@unibo.it (L. Mentaschi), zedd2@iacm.forth.gr (N. Chrysoulakis), parastat@iacm.forth.gr (D. Parastatidis), joachim.maes@ec.europa.eu (J. Maes).

https://doi.org/10.1016/j.scs.2021.103564
Received 6 September 2021; Received in revised form 19 November 2021; Accepted 19 November 2021
Available online 27 November 2021

the land surface, retrieved through satellite or airborne sensors data. The advantage of the use of air temperature measurements consists in the fact that they can provide representative and temporally continuous UHI information, but the presence of weather stations on the territory is often limited. On the other hand, estimating LST allows a spatially explicit analysis of temperature, but nevertheless is an indirect estimate of UHI, the so-called "Surface Urban Heat Island" (SUHI) (Clinton & Gong, 2013; Oke, Mills, Christen & Voogt, 2017). LST-based studies are increasingly common, due to the practical applications, immediacy and availability of sensors at no cost, particularly when there is the necessity to carry on analyses at regional or even global scale (Ottlè et al., 1992).

It is known that UHI exerts a detrimental impact on human health and quality of life in cities (Koppe, Kovats, Jendritzky, Menne & Breuer, 2004), particularly during heat waves.[1] Furthermore, the frequency and severity of heat waves have been on the rise over the last decade (Mishra, Ganguly, Nijssen & Lettenmaier, 2015). It is expected that this phenomenon will increase further in the future due to climate change, and it is thought that these changes are mainly driven by higher mean temperature rather than by temperature variability (Lhotka, Kyselý & Farda, 2018). In particular, heat waves have a projected increase in peak temperatures equal to 5 °C by the end of the century in Europe (Fischer & Schar, 2010). Moreover, the synergistic effect between heat waves and UHI, results in an increased energy demand for cooling systems in low and mid-latitude cities, which in turn adds to heat emissions and further raises temperatures in a positive feedback (Founda & Santamouris, 2017). On top of that, urbanization trend continues to grow worldwide, and in Europe as well, where the total artificial impervious area more than doubled from a 1990 baseline (Gong et al., 2020). On this aspect, Singh, Kikon and Verma (2017) demonstrated that urbanization and Land Use Land Cover change that occurred in Lucknow City, India, from 2002 to 2014, have led to an increase in temperature equal to over 1 °C, from an average of 36.7 to 37.8 °C. Similarly, Zhang, Estoque and Murayama (2017), estimated an increase of 1.64 °C from 2000 to 2013 in Nanchang City, China, in parallel to an increase of the urban area equal to 7260 hectares.

In this context, the deployment of Urban Green Infrastructure (UGI), which is defined as "a strategically planned network of natural and semi-natural areas with other environmental features designed and managed to deliver a wide range of ecosystem services" (European Commission, 2013), is recognized as one of the most important strategies to mitigate UHI and to promote a resilient environment in cities (Saaroni, Amorim, Hiemstra & Pearlmutter, 2018), since UGI provides the Ecosystem Service (ES) of microclimate regulation (CICES 2.2.6.2, Haines-Young & Potschin, 2018), amongst other services. Urban vegetation is in fact known to be an effective strategy to reduce heat intensity. Interestingly, O'Malley, Piroozfar, Farr and Pomponi (2015) found out trees, shrubs and grass to be the most effective UHI mitigation strategy, compared to other measures such as urban inland water bodies and high albedo materials. There are two main processes through which vegetation can mitigate heat: the shading effect, which consists in the interception of the solar radiation by leaves (radiative cooling), and evapotranspiration, which converts part of the energy stored in the urban canopy into turbulent fluxes of sensible and latent heat (evaporative cooling) (Chrysoulakis et al., 2018). The cooling capacity of UGI can vary largely and differs among vegetation types such as grass, shrubs and trees, reaching the maximum effectiveness with urban forests (Yoshida, Hisabayashi, Kashihara, Kinoshita & Hashida, 2015). It is known in fact that this process depends on plant structure, its physiological characteristics such as transpiration rate, and the amount of water intercepted and subsequently evaporated from the leaves (Rahman, Armson & Ennos, 2015), as well as on canopy size and tree density (Shashua-Bar & Hoffman, 2000). Healthy ecosystems and UGI can represent effective Nature Based Solutions (NBS) against the dramatic effects of UHI and climate change in cities, enhancing resilience and aiding to cool urban areas and preventing hazards such as heat waves. The unfolding of the European Green Deal (Von Der Leyen, 2019) and the European Biodiversity Strategy for 2030 (European Commission, 2020) poses an opportunity and a call to action in order to strengthen urban resilience and commitments on UGI. The adoption of an integrated planning aimed to the implementation of UGI to counteract the harmful effects of UHI can also represent an opportunity to meet multiple United Nation's 2030 Sustainable Development Goals, such as ensuring healthy lives and well-being for urban dwellers, improving urban resilience, reducing risks associated to climate change and sustainably manage ecosystems and biodiversity. This is also in close relationship with the fulfilling of the New Urban Agenda scope of achieving a sustainable, equitable, and fair environment for generations to come (European Commission, 2019; 2020; Von Der Leyen, 2019). The benefits that population can receive from such climate adaptation opportunities are dependent on the conservation and restoration of urban and peri-urban ecosystems. Nevertheless, despite the knowledge of the benefits that NBS (Somarakis, Stagakis & Chrysoulakis, 2019) can produce on a health, environmental, economic and social perspective, such benefits are often hindered by an unsustainable management and poor green urban planning occurring in many urban areas. Consequently, a substantial proportion of urban population currently lives in areas with potentially high heat exposure (EEA, 2020). For this reason, there is a need to systematically integrate UGI and NBS into urban planning, but in order to do so, science-based, spatially-explicit, widely available, and easily accessible information (Zulian et al., 2021), as well as studies on the role of vegetation cover and evapotranspiration, in different environmental contexts are needed (Qiu et al., 2017). In this context, Tiwari et al., (2021) point out the need of studies assessing quantitatively the impacts of UGI strategies on the ES of microclimate regulation in cities, as highlighted by previous research, as well as the need of high-resolution maps, in order to guide policymakers on the most appropriate measure to counteract UHI with NBS. In such regard, the new document "Evaluating the impact of Nature-based Solutions: a handbook for practitioners" is hot of the press. It is an enormous collaborative effort of 17 EU Horizon 2020 projects to provide practitioners with a comprehensive NBS impact assessment framework, and a robust set of indicators and methodologies to assess impacts of NBS (European Commission, 2021).

Several studies have highlighted the benefits of vegetation patches inside urban areas to cool summer temperatures. Jansson et al. (2007), estimated that the air temperature difference between a park and the built-up area in the city of Stockholm, Sweden, is in the range of 0.5–0.8 °C, with a maximum of 2 °C, whereas Wang and Akbari, (2016)) showed that street trees can cool air temperature by 0.2–0.3 °C in the city of Montreal, Canada. Furthermore, Venter et al. (2020), estimated that each city tree in Oslo, Norway, has the potential to mitigate heat exposure for one citizen by one day. As regards wider spatial contexts, Heris et al., 2021 developed an urban ecosystem account framework for 768 U.S. cities, estimating the heat mitigation role of urban trees and the related cooling energy savings for a total value of around 4098 and 4229 GWh in 2011 and 2016, respectively. Furthermore, Mentaschi et al. (2021), developed a global long-term dataset of urban-rural surface temperature differences at high resolution.

Most studies evaluated the ES of microclimate regulation at city and neighborhood scale and there are fewer studies investigating the phenomenon at regional or continental scale, in particular in Europe. In fact, the majority of these studies are carried out at city or regional level, and analyze only particular UGI elements such as parks (Saaroni et al., 2018), making it difficult to generalize on the overall role of vegetation in mitigating urban temperatures in cities. In this regard, a more integrated methodological framework encompassing multiple scales and across large areas is needed (Bartesaghi-Koc et al., 2018). A limitation of more large-scale studies is often represented by the lack of air

[1] A heat wave is a period of unusually hot weather that typically lasts two or more days. To be considered a heat wave, the temperatures have to be outside the historical averages for a given area (https://scijinks.gov/heat/)

temperature data. This is particularly true for small towns, where weather monitoring stations are often missing (Tiwari et al., 2021). This inherent difficulty leads to the necessity to resort to coarse-level spatial air temperature models, which often cannot grasp the peculiar heterogeneity inside urban areas. Another alternative is the use of satellite-derived LST which only provides an indirect estimation of the UHI effect. A combination of the two approaches is therefore desirable, allowing to benefit from the respective advantages (Schwarz et al., 2012). On this aspect, Bartesaghi-Koc et al. (2018), observed that a more holistic approach encompassing the dynamic spatial heterogeneity of urban areas, as well as the reciprocal cumulative effects of natural and anthropic features is needed. Furthermore, they also suggest expanding the research related to the effect of evapotranspiration in urban areas in relation to temperature reduction; in fact, the majority of studies focused more on structural features of UGI while analyzing their thermal impact on cities, often overlooking their functional aspects related to evaporative cooling. Finally, it appears clear that, despite the growing body of studies on UGI and UHI, there is still the need for more easily accessible evidence for policymakers, in order to provide indicators and information that can be practically integrated into urban planning and legislation (Bartesaghi-Koc et al., 2018).

Due to the growing urban population and the current and projected risk posed by UHI and climate change, this study estimates the role of urban and peri-urban vegetation in mitigating air temperature in cities, that is, the microclimate regulation ES. For this purpose, a high-resolution, spatially-explicit model which estimates the cooling capacity of vegetation at urban continental level, in particular in 601 Functional Urban Areas (FUAs) in the EU-27, has been applied. The role of vegetation has been predicted on the basis of its spatial extension and canopy transpiration, with an approach that couples both air temperature and LST data. This quantitative approach allowed to calculate the temperature difference between a baseline and a no-vegetation scenario, for each FUA. Then, a policy-support oriented indicator has been developed, in order to be available by city administrations or stakeholders, which allows to evaluate the amount of vegetation that is needed in the city to lower temperature by a certain extent.

2. Data and methods

2.1. Study area

The role of UGI in reducing air temperature has been estimated for 601 Functional Urban Areas (FUAs) in the EU-27. FUAs, formerly known as Larger Urban Zones (LUZ), defined in 2011 by the European Commission and the OECD, are developed by Eurostat as part of the urban administrative statistical units. The FUAs allow to map and evaluate the city and its immediate surrounding and a comparative analysis of cities amongst the Member states. They are represented by the core city and its commuting zone and are used to describe the European urbanized land, as recommended by Eurostat (Dijkstra & Poelman, 2012; EuroStat, 2016; Eurostat, 2017). Data has been downloaded from the Eurostat website (Eurostat, Urban Audit, 2020, version 2018) and is structured as follow:

- Functional Urban Areas, defined as the core city (with at least 50,000 inhabitants) and the commuting zone. FUAs represent an 'operational urban spatial extent' that allows mapping and evaluating the city and its surroundings.
- Core cities are cities with at least 50,000 inhabitants. One FUA can include one or more core cities. As reporting unit for core cities, all core cities within the same FUA have been aggregated.
- Commuting zones are transition areas, from agricultural or semi-natural to urban land use and are very important when considering ES. This definition is based on commuter's behavior, employed persons living in one city and working in another city. Occasionally, FUAs do not include a commuting zone, if the municipalities around a core city do not meet the necessary criteria (15% of the cases).

2.2. LST retrieval

The process to estimate LST from satellite data relies on the availability of thermal infrared sensors. Satellites such as Landsat 5, 7 and 8 are suitable for estimating LST. In this case, Landsat-8 OLI TIRS data have been used. LST data have been acquired through the Google Earth Engine (GEE) platform, using a single channel algorithm developed by Parastatidis et al. (2017). The algorithm analyzes Landsat thermal bands and relies on different emissivity sources: i) a global emissivity map derived from ASTER (Advanced Spaceborne Thermal Emission and Reflection Radiometer) data at a 100 m spatial resolution; ii) the MODIS (Moderate Resolution Imaging Spectroradiometer) daily LST/emissivity product (1 km spatial resolution); and iii) vegetation fraction-based emissivity, estimated from NDVI (Normalized Difference Vegetation Index). In the GEE environment, the median summertime LST (1st July-31st August 2018) has been calculated and extracted in correspondence of the FUA boundaries.

2.3. Air temperature dataset

Because of the lack of high-resolution air temperature datasets at European scale and due to the insufficient coverage of the existing weather stations network, a dataset elaborated by the University of Colorado Denver, derived from NOAA (National Oceanic and Atmospheric Administration) weather stations network daily measurements in the U.S (Heris et al., 2021) have been used to build a predictive model of the relationship between surface temperature and air temperature of the EU FUAs.

The dataset consists of more than 6500 records of maximum summertime air temperature (June 15th to August 15th) from weather stations, comprises their latitude and longitude, and the average LST of each station's neighborhood (using a buffer of 1 km).

This dataset is trained by the LST, land cover types, average relative humidity, elevation, and precipitation to estimate air temperature. Incorporating a wide range of variables makes it suitable for contexts outside of the U.S.

2.4. Population

In order to assess the benefit of the temperature mitigation ES received from urban dwellers, the share of population residing in areas where the microclimate regulation occurs, i.e. where the cooling is positive, has been estimated, and expressed in percentage. For such purpose, the Global Human Settlement layer population density dataset for 2015 (release year: 2019; Freire et al., 2019; Schiavina, Freire & MacManus, 2019), expressing the distribution and density of residential population has been used.

2.5. Microclimate mitigation model

The biophysical model is based on an adaptation of a two-level method reported in Heris et al., 2021: in the first level, a bivariate linear regression model has been developed to estimate LST, using tree cover density and the amount of water evaporated from tree canopies as predictors. Then, a second univariate model has been developed to estimate maximum air temperature as a function of two predictors: the LST estimated through the first regression model and latitude. Finally, the two models have been coupled to calculate the cooling capacity of vegetation. The model has been run, pixel-wise, in all European Functional Urban Areas (FUA) in the EU-27 (Eurostat, Urban Audit, 2020), between July to August (year 2018) in a Python environment. The summer season has been chosen for two main reasons: first, it is known that the UHI phenomenon and related cooling mechanism are more

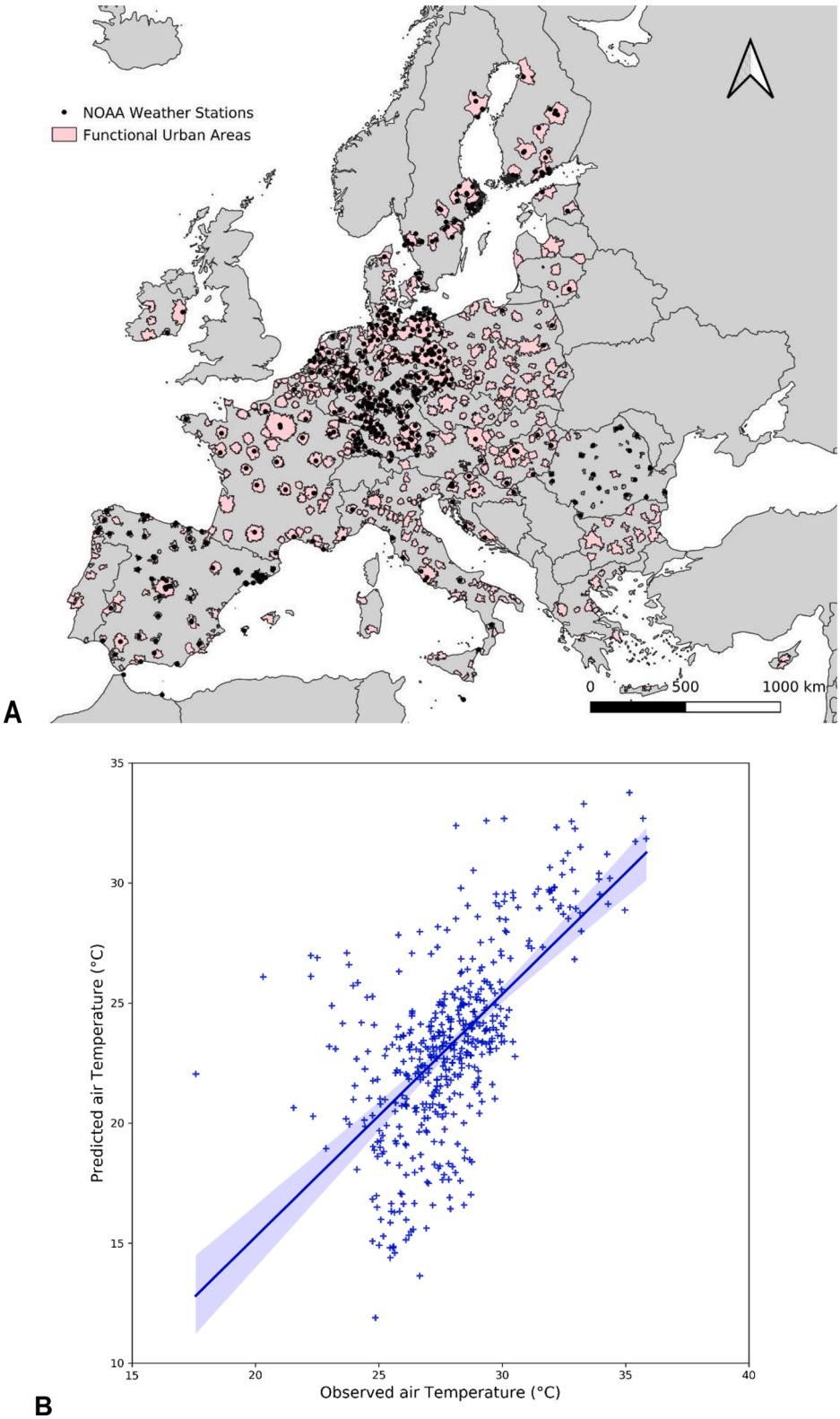

Fig. 1. Distribution of the Functional Urban Areas and of the NOAA weather stations monitoring network (A) and plot of the microclimate regulation model validation (B). Observed air temperature data used in the validation, is derived from 463 records of maximum air temperature from the NOAA weather stations (July-August 2018). Adjusted R^2: 0.4; RMSE: 0.15; Scatter Index: 26%, Bias: 4.66. Both intercept and slope are significant for $p \leq 0.05$.

pronounced in the summer; and secondly, data availability due to less cloud cover. Due to the different spatial resolution of the input datasets, they have all been resampled to a common pixel size in order to ensure geometrical consistency. Therefore, all the elaborations have been performed at a spatial resolution of 100 × 100 m. The output of the model is presented as the average cooling at FUA level. Nevertheless, for each city, a map with cooling capacity computed at high resolution is available. The steps of the model are detailed below:

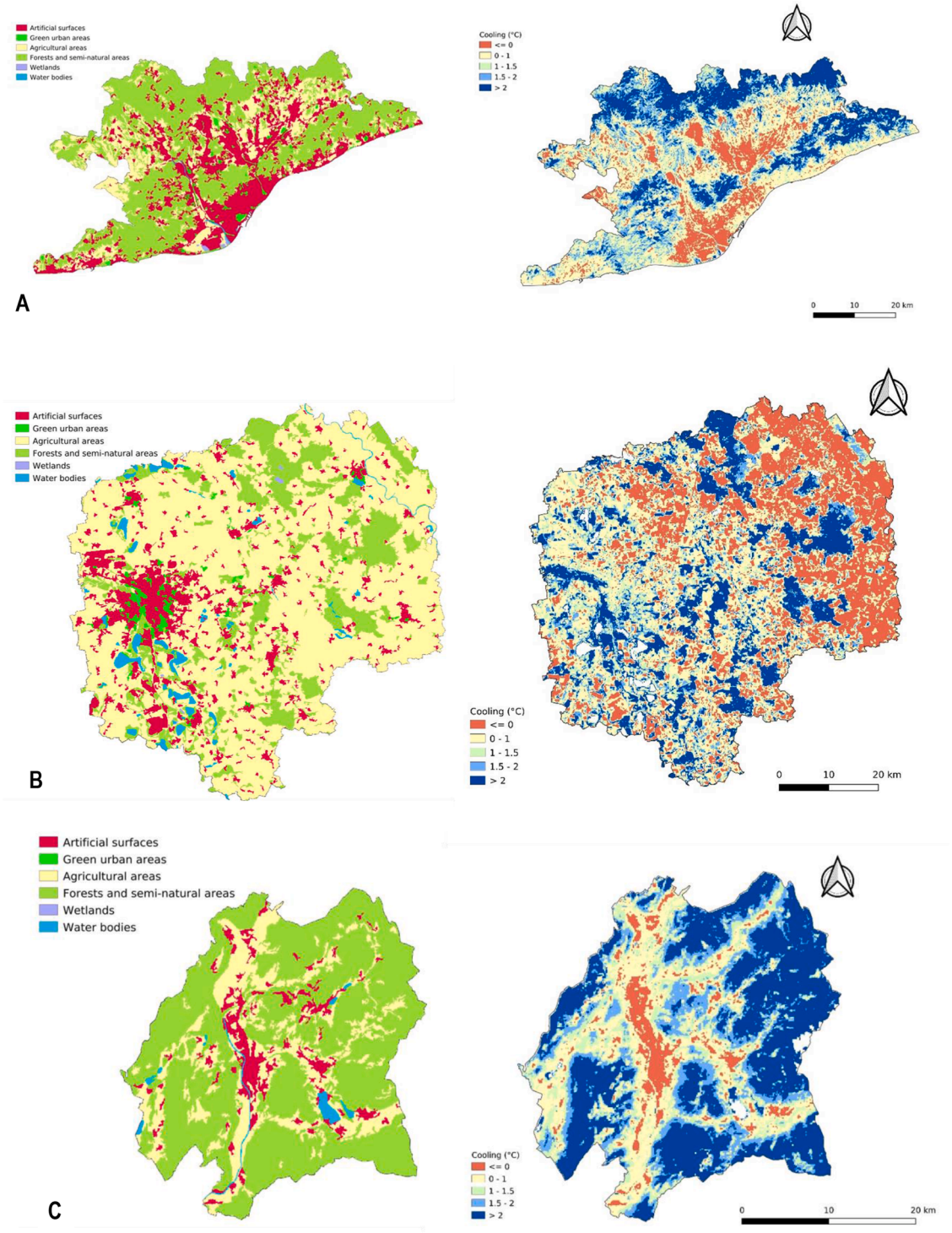

Fig. 2. Cooling and land cover maps in three FUAs: Barcelona, Spain (A), Leipzig, Germany (B), and Trento, Italy (C).

(i) First, Landsat 8 OLI/TIRS images have been used to compute the median LST (July-August 2018) through a single channel algorithm implemented in Google Earth Engine (GEE) by Parastatidis et al., (2017).

(ii) Then, for every city, a linear regression model has been run to predict LST (°C) in function of variables related to urban vegetation, at pixel level, with an ordinary least square algorithm implemented in the Python package Statsmodels. In order to do so, tree cover density (Tc) (from Copernicus High Resolution Layer, year 2018) and the amount of water evaporated from tree canopies (E_{tree}, mm day^{-1}), expressed as the sum of transpiration (E_c, mm day^{-1}) and vaporization of intercepted rainfall from vegetation (E_i, mm day^{-1}) (from PML V2 evapotranspiration product, based on the Penman-Monteith-Leuning canopy conductance model, Gan et al., 2018; Zhang et al., 2019) have been selected as independent variables, as can be seen in the general equation of the bivariate regression (Eq. (1)). The total evapotranspiration has not been included since, after a fist evaluation, evaporation from the soil proved to be a confounding factor, not strictly related to vegetation.

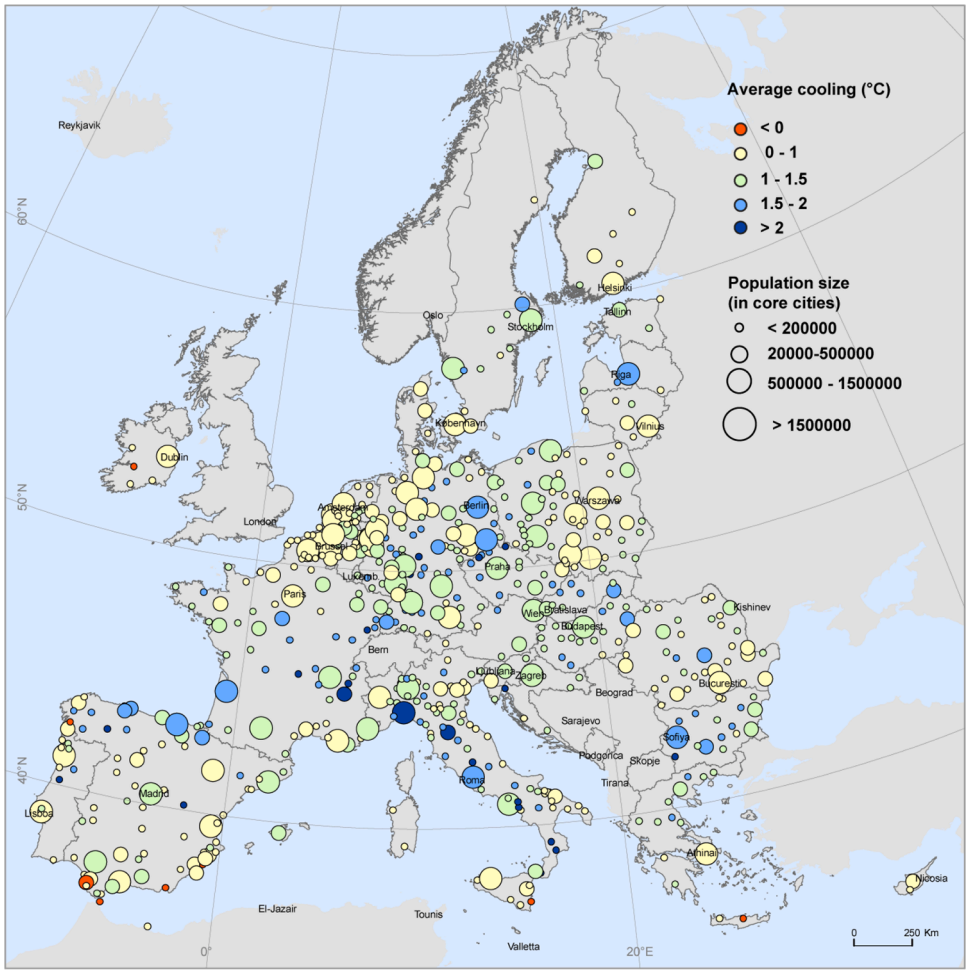

Fig. 3. Map of average cooling (°C) in EU 27, 2018.

$$LST = \beta_{0e1} + \beta_{1e1} Tc + \beta_{2e1} E_{tree} \quad (1)$$

(iii) After that, a second ordinary least square model, trained with the air temperature dataset, allowed to predict maximum air temperature (Tair, °C) on the basis of LST and latitude:

$$Tair = \beta_{0e2} + \beta_{1e2} LST + \beta_{2e2} Latitude \quad (2)$$

(iv) Then, a value of zero has been assigned to Tc and E_{tree} to estimate LST in a no-vegetation scenario (LST_0, Eq. (3)). Then, the two regression models have been coupled (Eq. (4)) to estimate the impact of trees on air temperature reduction for the no-vegetation scenario.

$$LST_0 = \beta_{0e1} + \beta_{1e1} Tc_0 + \beta_{2e1} Etree_0 \quad (3)$$

$$Tair_0 = \beta_{0e2} + \beta_{1e2} LST_0 + \beta_{2e2} Latitude \quad (4)$$

(v) It was then possible to estimate, for each 100 × 100 m pixel, the difference between the temperature of the no-vegetation scenario and the temperature estimated in correspondence of vegetated areas, obtaining the cooling capacity of vegetation (°C), hereafter referred to as "cooling" (Eq. (5)). The cooling has subsequently been averaged at FUA level to obtain the average cooling for each city.

$$Cooling = Tair_0 - Tair \quad (5)$$

The elaborations have been computed using the following open-source software: Spyder 4.1 and Grass GIS v. 7. Some FUA have been excluded from the analysis due to inadequate or lacking data (total of FUA analyzed: 601). Furthermore, since the focus of the study is the temperature reduction on land from vegetation, water bodies have been excluded from the analysis.

2.6. Cooling index

Here, in order to make results on cooling operative as a policy-support instrument, a cooling index, which standardizes and aggregates the information included in the output of the microclimate regulation model, is proposed. The results of the model, averaged at FUA level, have been analyzed to estimate an empirical relationship between the different variables employed in the model, in order to evaluate the amount of urban vegetation needed to reduce temperature by a certain extent. The scope of the cooling index is not to further examine analytically the UHI phenomenon, but to provide a practical tool that can be easily employed for policy or research purposes.

2.7. Analysis of the drivers of cooling

Finally, we have analyzed whether there are significant differences between countries in relation to the relationship between temperature reduction and ratio of green infrastructure in each city. For this purpose, several regression models were investigated to estimate if the data

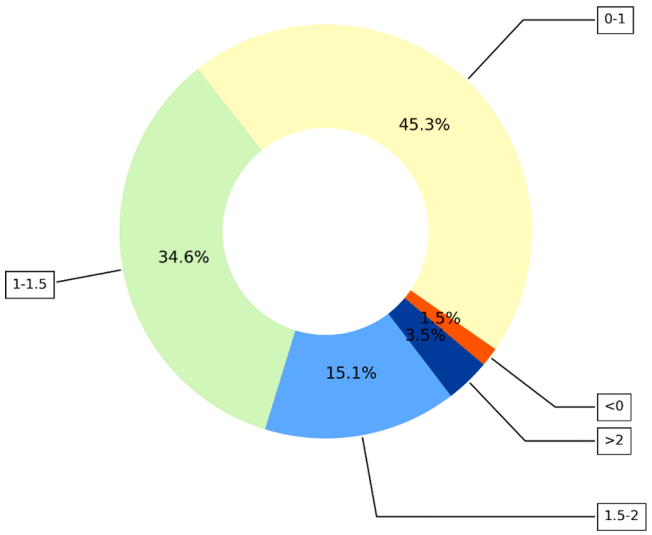

Fig. 4. Proportion of cities (%) with a different degree of cooling (°C).

contains global and group-level trends, specifically significant differences between the FUA of different countries, as well as to compare the explanatory capacity of the different variables. The considered predictors are the following: total amount of tree cover (% of the FUA), total E_{tree} (mm day^{-1}), elevation (m), population (number of inhabitants), city size (km^2), population density (inhabitant per km^2), city structure (dimensionless) and distance from the sea (m). The models were run on data from all 601 European cities using the software R studio.

2.8. Validation

In order to test the model predictions, average summer (July–August 2018) air temperature records from 463 weather stations of the NOAA network, located in the EU-27 territory, have been used to validate the air temperature estimated through the model. The value of each estimated air temperature pixel has been sampled in correspondence of the location of each weather station, and then regressed against the corresponding observed air temperature values. Adjusted R^2, RMSE, Scatter Index and model coefficients have been calculated to assess the accuracy of the model.

2.9. Error propagation

The uncertainty of the model has been estimated by calculating propagated error of the two regressions, for each city. In order to do so, Taylor (1997) method for accumulated prediction fractional uncertainties has been taken into account. Fur such a purpose, Eq. (6) has been applied:

$$Propagated\ error = \sqrt{\left(\frac{\delta_{Ta}}{|Ta|}\right)^2 + \left(\frac{\delta_{LST}}{|LST|}\right)^2 + \left(\frac{\delta_{Ta_0}}{|Ta_0|}\right)^2 + \left(\frac{\delta_{LST_0}}{|LST_0|}\right)^2} \quad (6)$$

Where δ is the error, Ta is the estimated air temperature, LST is the land surface temperature, and Ta_0 and LST_0 are the estimated air and surface temperature for the no-vegetation scenario, respectively. The errors (δ) have been calculated through the average of the observed upper and lower confidence interval (alpha = 0.05) values from cell-level predictions (Frost, 2017).

3. Results

3.1. Microclimate regulation model

The model validation (Fig. 1) yielded an adjusted R^2 equal to 0.4 and a RMSE% of 0.15. The Scatter Index is equal to 26% and the predicted air temperature is slightly biased towards lower values.

In Fig. 2, the cooling maps of some of the cities (A: Barcelona; B: Leipzig; C: Trento) are shown. The areas characterized by cooling values below zero are mainly urbanized, where impervious surfaces and agricultural areas are prevalent, whereas higher cooling values can be observed in correspondence of more natural and sparsely vegetated areas.

Regarding the cooling aggregated at FUA level, the average European cooling is equal to 1.07 °C, with an average minimum of −3.27 °C and an average maximum of 5.21 °C. The median R^2 of the first regression (Eq. (1)) of the microclimate regulation model is equal to 0.44, with the majority of cities displaying a R^2 over 0.4. The overall performance of the first regression is reported in Table A.2 of the Appendix. The average value of the propagated error is 0.5. In Fig. 3, the map of the average degree of cooling (°C) in EU27 FUAs is presented. The average degree of cooling ranges from negative values (−0.4 °C) up to 2.9 °C. Proportional circles express population size in core cities. A few cities displaying an average cooling below zero are present in coastal areas of southern Europe, in particular Spain, Italy and Greece. Cities with an average degree of cooling between 0 and 1 appear to be concentrated in southern regions as well, other than Belgium, Netherlands and Poland. Cities with an intermediate degree of cooling (1–2 °C) are more widespread and present particularly in continental Europe, whereas cities with a high degree of cooling (> 2 °C) can be seen in Italy along the Apennines, and in the most continental areas.

Overall, these cities with a high degree of cooling represent the 3.5% of the total of the FUAs (Fig. 4), whereas 15.1% of the cities display an average cooling between 1.5–2 °C, 34.6% within 1–1.5 °C, and 45.3% are within 0–1 °C, whether only 1.5% of FUAs display a cooling below zero.

Fig. 5 shows the share of FUA area (%) characterized by different cooling intervals (°C) in EU capital cities. Dublin has the highest amount of city area displaying a negative degree of cooling (around 37%) as well as other large Capital cities such as London: (31%) Copenhagen (31%) and Athens (31%). These cities are also amongst the cities with the lower proportion of high cooling (above 2 °C), together with Bucharest, Vilnius, Amsterdam and Warsaw (below 10% of the city area). On the other hand, Ljubljana (which has also been European Green Capital in 2016), Zagreb, Stockholm and Riga show less than 8% of the city area with a cooling below 0, whereas cities like Sofia, Rome and Riga, have the highest city area with a cooling over 2 °C (around 45%, 43% and 42%, respectively).

Then, several regression models have been tested to evaluate differences between EU countries. Out of the models examined, a multiple linear regression with a country-specific fixed effect has been selected as the most appropriate for this scope (Appendix A, Fig. A. 2). A comparison of all the models evaluated can be found in Appendix A, Table A.1. As expected, the most important explanatory variable for predicting the cooling factor was tree cover. The model works well for all countries except the northernmost countries such as Finland and Latvia. Within the most significant countries, it can be seen how for the Mediterranean ones (ES, PT) the model tends to predict higher than expected values for high cooling values, and in some extent, also to underestimate the cooling for low values. Lastly, Fig. 6 shows the amount of population, expressed in percentage of the total population residing in a FUA, which benefits from the microclimate regulation service, by country. 63% of the countries show a share of beneficiaries over 50%, with Hungary and Cyprus displaying the highest proportion of beneficiaries (over 80%, median value), followed by Czech Republic and Bulgaria, with a median of around 80%. Finland and Ireland have the lowest percentage of

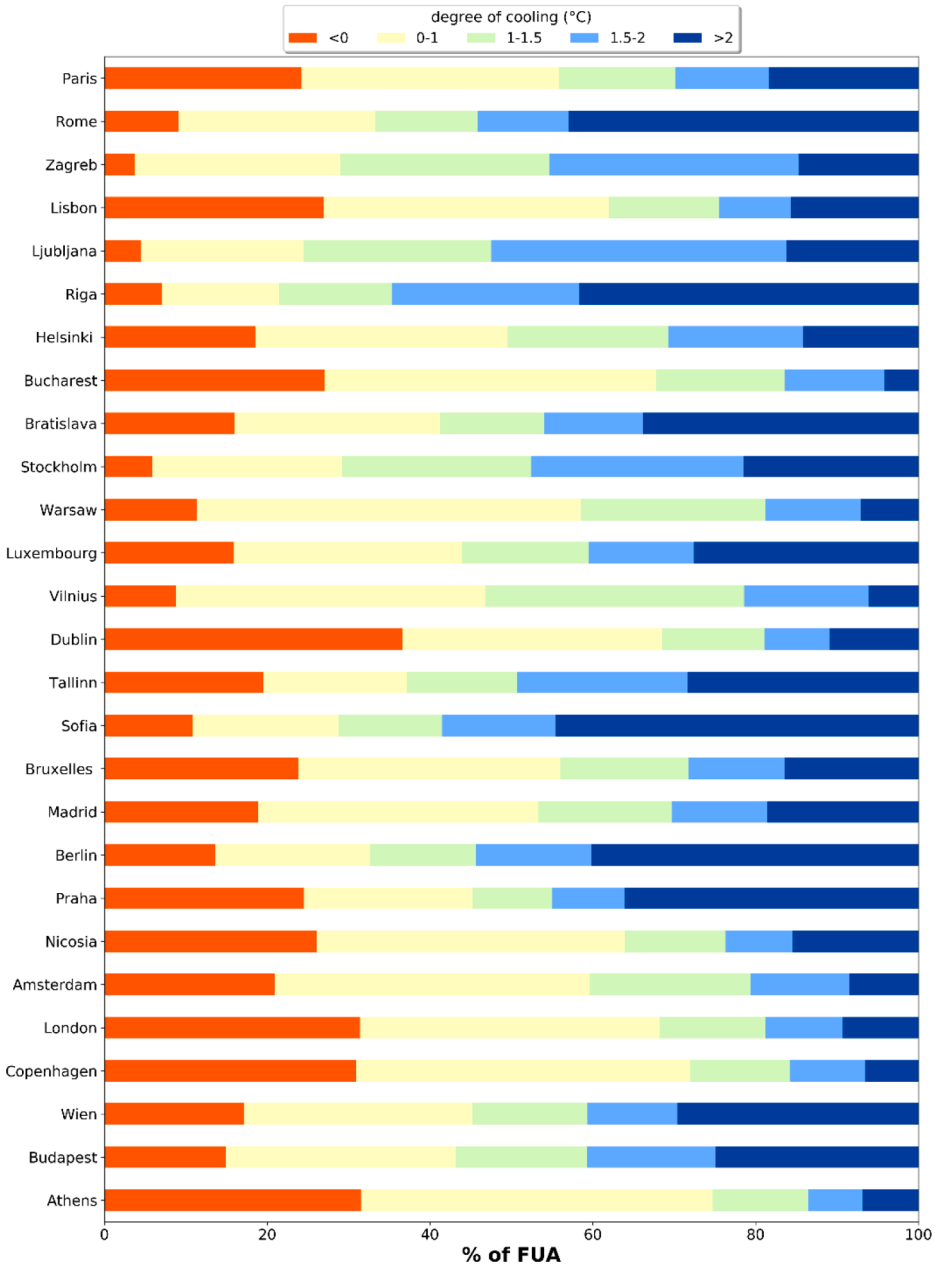

Fig. 5. Percentage of FUA for different cooling intervals (°C) in EU capital cities.

population benefiting from the microclimate regulation, with a median value of only 21% and 16%, respectively. Countries such as Spain, Greece, Italy, Denmark and France show a high variability, cities are extremely diverse in their response to urban heating, with the amount of beneficiaries ranging from less than 10% up to almost 100%.

3.2. Cooling index

The average cooling at FUA level has been combined in an analytical equation together with two relevant city-scale variables: tree cover and average LST. Hence, an empirical relationship has been derived, and the average cooling capacity of vegetation (in °C) at FUA level can be expressed in form of an index (hereafter referred to as Cooling index, CI). The CI has been derived as follows:

$$\mathrm{CI} = \frac{Tc \times T_{mean}}{i \times 100} \tag{7}$$

Where Tc is the tree cover, which expresses the percentage of vegetation inside a city (%), T_{mean} is the average summer land surface temperature (°C) in the summer period, and i is an empirically-derived constant (dimensionless) equal to 5, and 100 is a correction factor. It has been estimated on the basis of the average trend of the model and expresses the relationship between vegetation and urban temperature. Eventually, Eq. (7) can be reversed, placing the Tree Cover as the unknown variable, in order to express it as a function of CI, so that the administrators can obtain the amount of vegetation that is needed to cool the city by a certain degree, replacing CI with the desired degree of cooling:

$$\mathrm{Tc} = \frac{CI \times i \times 100}{T_{mean}} \tag{8}$$

The Cooling Index allows to generalize the relationship between the cooling effect, and the amount of vegetation inside a city, in order to directly derive the Cooling without the need to calculate it for each city with our model. This makes the Cooling Index a suitable tool for

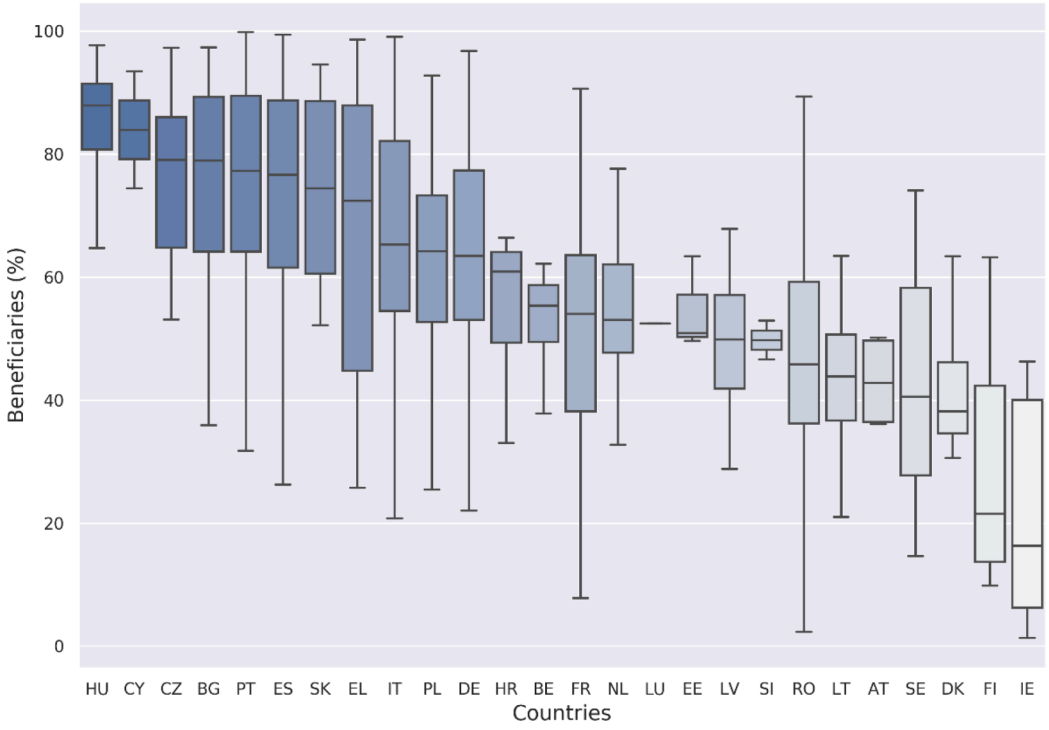

Fig. 6. Number of beneficiaries (expressed as the percentage of population residing in urban areas where the cooling effect of vegetation occurs) per country (AT: Austria; BE: Belgium; BG: Bulgaria; CY: Cyprus; CZ: Czech Republic; DE: Germany; DK: Denmark; EE: Estonia; EL: Greece; ES: Spain; FI: Finland; FR: France; HR: Croatia; HU: Hungary; IE: Ireland; IT: Italy; LT: Lithuania; LU: Luxembourg; LV: Latvia; NL: Netherlands; PL: Poland; PT: Portugal; RO: Romania; SE: Sweden; SI: Slovenia; SK: Slovakia).

Table 1
relationship between the percentage of tree cover within a FUA and degree of cooling (°C).

Degree of cooling (°C)	Tree Cover (%)
1	16
2	32
3	48

policymakers and stakeholders to estimate and monitor the performance of a city's green infrastructure in reducing summer temperatures. Since the indicator has been developed in a range of cooling up to 2.9 °C, cooling values outside this range cannot be inferred. The average LST and tree cover of a city are easily available, city administrators or stakeholders can estimate the CI at FUA level, either calculating the current cooling capacity of the city, or estimating the required tree cover to obtain a certain degree of cooling. The cooling index represents the slope of a linear relationship between tree cover and cooling. By applying the cooling index in the FUAs examined, it is possible to observe how a decrease by 1 °C on average in a FUA, corresponds to a tree cover of 16%. Accordingly, a 2 °C and 3 °C cooling correspond to a 32% and 48% of tree cover, respectively (Table 1).

4. Discussion

In this study, we assessed the microclimate regulation ES across different European FUAs, providing a measure of the role provided by UGI in mitigating the UHI effect. Mapping and quantifying urban ES at continental scale is a challenging task due to the different climatic, cultural, socio-economic, and environmental characteristics, as well as due to the intrinsic heterogeneity of urban areas. This heterogeneity often represents a hinder to a proper estimation of ES, especially when synthetizing observation at city level, due to the inherent complexity of urban ecosystems and the interplay of different confounding factors. However, the proposed approach has already proven to be suitable and efficient in characterizing microclimate regulation in 768 urban areas in the US (Heris et al., 2021), and in the present study, where 601 FUA of different sizes and morphologies and have been examined at high resolution. These results expand the work previously carried out in the context of initiatives promoted by the European Commission, namely the MAES process (Mapping and Assessment of Ecosystems and their Services, (Maes et al., 2016), as well as the EnRoute Project (Maes et al., 2019; Zulian et al., 2018). In such a context, a framework aimed to obtain spatially explicit information can identify areas inside cities that would benefit the most from targeted greening intervention aimed to reduce excessive temperatures and ameliorate living conditions of urban dwellers. The average cooling for all EU is 1.07 °C, which is in line with what reported in other studies (Oke, 1987; Tsiros, 2010). The majority of cities has an average cooling within 1.5 °C, and only a small fraction has a high cooling from vegetation. It should also be noted that some FUA display an average cooling below 0 °C, in particular in some southern coastal areas of Spain and Italy. It is known in fact that a negative UHI, i.e. when the temperature difference between urbanized and vegetated areas is negative, can be present especially in arid regions in conditions of atmospheric stability (Alonso et al., 2003; Clinton & Gong, 2013; Sobrino et al., 2013). This phenomenon could be the results of a combination of factors: vegetation structure (grassy UGI can potentially have a higher temperature than the surrounding, in particular if they are not irrigated, (Potchter et al., 2006; Saaroni et al., 2015), environmental constraints of the Mediterranean area which can limit evapotranspiration through drought (Fusaro et al., 2015) and the share of shaded surfaces in urbanized cores, where the density and height of buildings is higher (Memon, Leung & Liu, 2009). In fact, it has been observed that in those cities, surface temperature was inversely related with tree cover. The occurrence of droughts is a common phenomenon in the Mediterranean, and also in more continental and northern countries recently due to climate change; therefore, the maintenance of an adequate water supply to UGI poses a dilemma in areas with water scarcity, and a trade-off must be considered (Nouri, Borujeni & Hoekstra, 2019). In other particular cases, such as at higher latitudes, this phenomenon could be due to a generally lower LST and to the high relative humidity of urban and peri-urban green areas, which result in a low latent heat flux and higher heat storage than artificial surfaces, due to the lower albedo of vegetation. Therefore, under specific

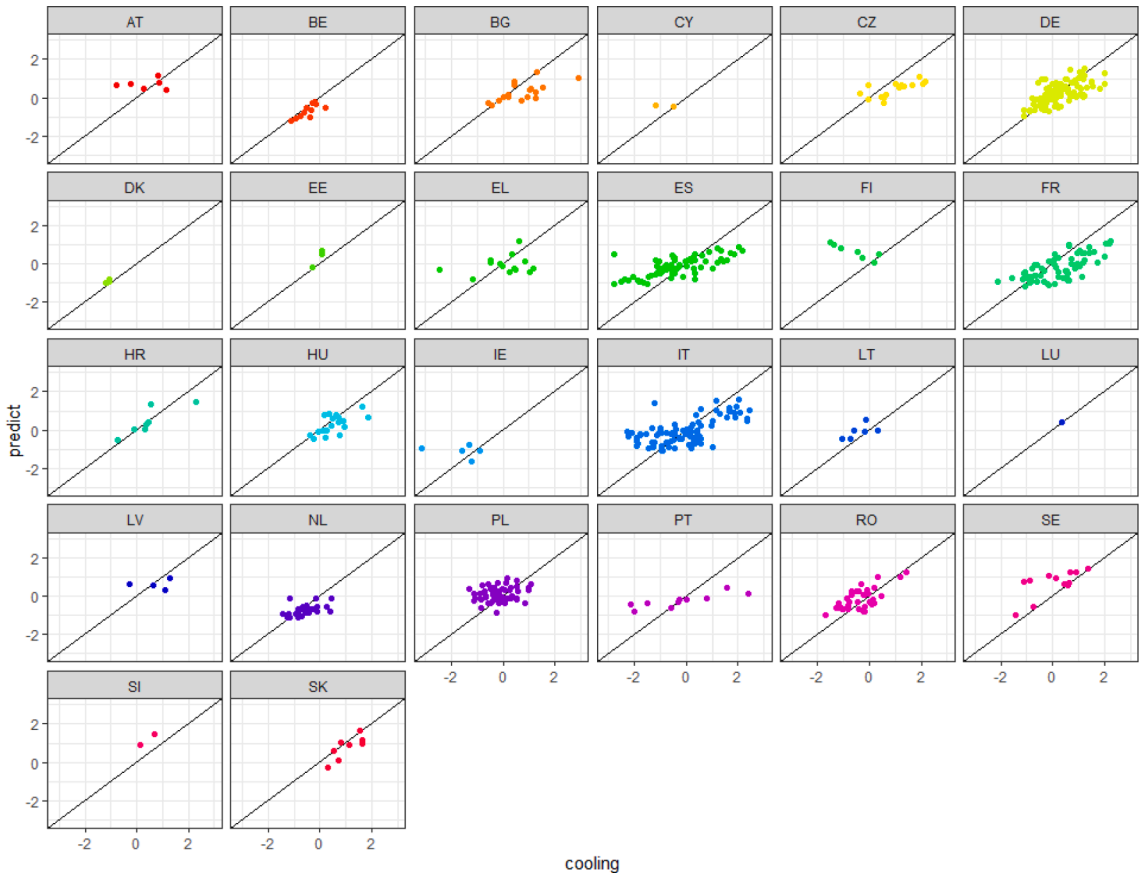

Fig. A.1. Cooling average estimation for the 601 European FUA, paneled by country computed with the multiple regression model M1.

circumstances, it is possible that pixels corresponding to vegetative areas have higher LST than the pixels corresponding to open non-vegetative areas in cities, which may lead to a low or even negative cooling index (Karnieli et al., 2019; Manoli, Fatichi et al., 2020). The study aided also to identify which are the main factors that maximize this ES. In our model, tree cover and transpiration appeared to be the most important predictors of urban air temperature, regardless of city characteristics. However, some differences across different countries are present: in northernmost countries such as Finland and Latvia, it is possible that the UHI phenomenon is not clearly observable, at least in these current study-specific conditions. Otherwise, it is also possible that the considered predictors do not reflect well the thermal dynamics in place in these areas, where peculiar territorial and physical characteristics occurs, such as the typical Finnish peatbog landscape. On the other hand, it is interesting to see that in southernmost countries such as Portugal and Spain, the model overestimates the cooling for high values, indicating that in these countries, environmental constrains are in place, which limit the efficiency of provision of ES in comparison to the average behavior of UGI in other countries when tree cover is highest, such the aforementioned drought conditions. Hereby, it is possible to derive that the extent (expressed as% of the total reporting unit) and the transpiration rate of vegetation are crucial in providing microclimate regulation in cities. This is also visible from the maps, where the highest cooling can be observed in correspondence of densely vegetated areas, being the case for parks inside the core city, or more peri-urban forested areas. It is known in fact, that the extent of UGI in an urban area exerts an influence on UHI magnitude (Yu et al., 2017). This has also been observed in a previous study for the city of Rome (Marando et al., 2019), where the surface covered by trees, as well as NDVI, demonstrated to be the most important factors in reducing summer temperatures. Similarly, Bokaie et al., (2016), highlighted a negative correlation between LST and vegetation and green spaces in the Tehran Metropolitan City. Contextually, it is important to underline that urban and peri-urban vegetation, can exert a different role in mitigating summer temperatures. It has been highlighted, in fact, that peri-urban forests are more effective in providing this ES, both in higher temperature reduction and cooling distance (Marando et al., 2019). In this context, city investments on UGI and land sustainability can ease multiple societal challenges, providing several benefits for urban dwellers (Maes et al., 2018; Manes et al., 2016). For this reason, the European Commission set up the Green City Accord initiative, where cities over 20,000 inhabitants are called to develop ambitious Urban Greening Plans by the end of 2021 in order to bring nature back to urban areas. The creation of connected, biodiverse and accessible UGI, in collaboration with the EU Covenant of Mayors, will have a central role in tackling the harmful effects of climate change and providing cleaner, healthier spaces for urban dwellers. Also, other European Commission initiatives on UGI have been set up in the last years, such as the EU Strategy on Green Infrastructure and the Action plan for nature, people and the economy (Zulian et al., 2021). This study allowed also to measure the burden that UHI has on population in different urban areas, providing a picture of the current condition in Europe. These results shed a light on the alarming situation on which citizens are subject to: the almost 40% of European countries have half of the population exposed to UHI effect. From a socio-demographic perspective, particular attention should also be posed to the most vulnerable population groups, such as those in poverty or the elderly population, since they are often the most affected (Morabito et al., 2015). Interestingly, Li et al., (2020) have evaluated that the most important predictor of UHI variation is NDVI. However, among the socioeconomic factors, the most significant contributor for UHI was urban economic scale, followed by population size and per capita GDP. Sebastiani et al., (2021) have indeed pointed out how UHI effect impacts

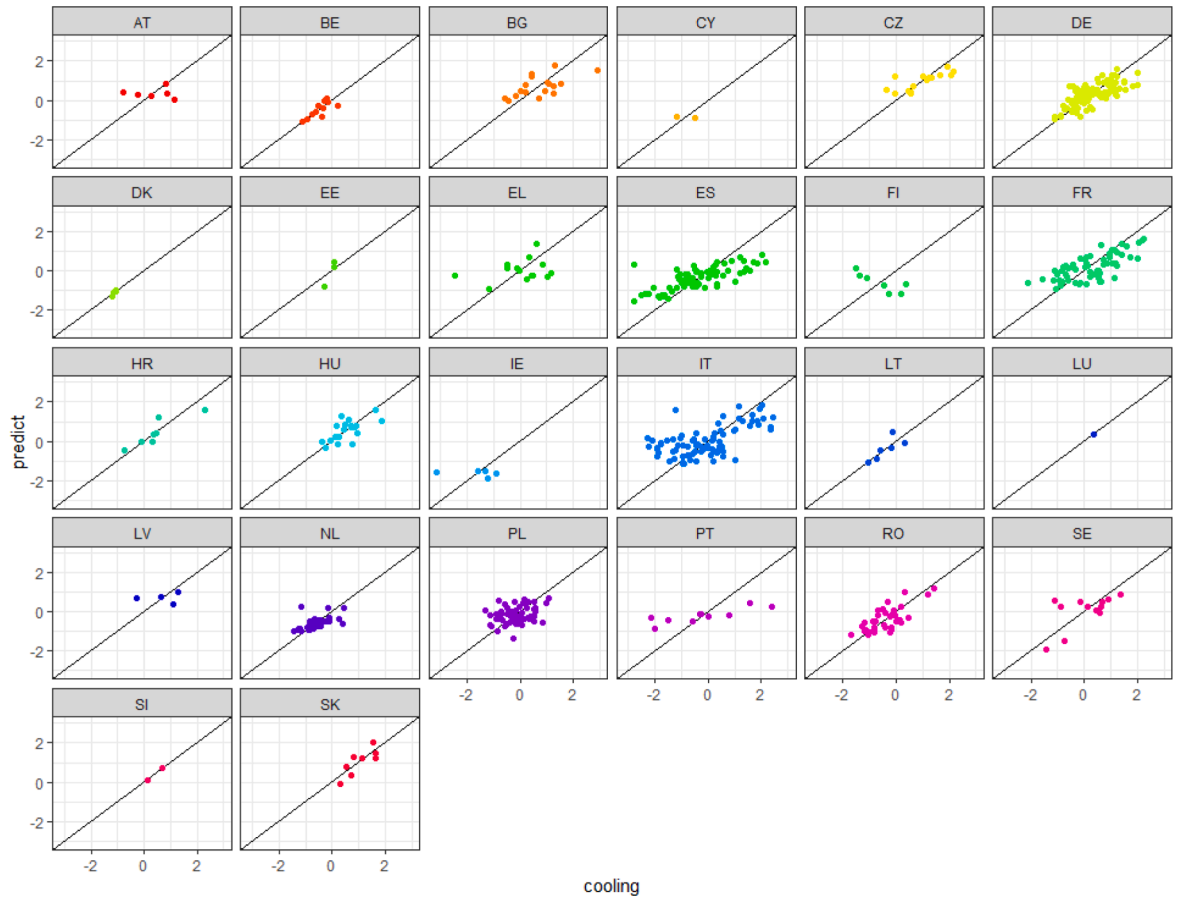

Fig. A.2. Cooling average estimation for the 601 European FUA, paneled by country computed with the multiple regression model M4.

the most areas with high degree of urbanization and population density, which corresponds to areas where the mismatch of this ES occurs, that is, where the detrimental effect of UHI is not compensated by nature and where the demand is higher. In this regard, efforts aimed to reduce the mismatch in this ES should be undertaken, especially in view of the expected exacerbation of UHI and heat waves events from climate change. Finally, the set of large-scale information provided by the model allowed to produce a simple and synthetic index that can inform urban planning and policy. Hereby a proposed tree cover of at least 16% per FUA is recommended in order to achieve a temperature reduction equal to 1 °C. This is in agreement with previous research carried out in Toronto, Canada, where an analogous relationship between tree canopy cover and temperature reduction at daytime was found (Wang and Akbari, 2016b). In this way, a larger proportion of citizens would benefit from the temperature mitigation, allowing to lessen the damage posed by extreme temperatures. Interestingly, Kondo et al. (2020) have found that up to 610 premature deaths can be prevented annually in lower socioeconomic status areas of Philadelphia, if the city tree canopy cover were increased up to 30%. However, in some European areas, forests have seen a reduction in their extent, and the process characterizes also cities in northern countries, entailing a loss in the potential of these ecosystems to reduce temperatures and to provide other ecosystem services. Furthermore, forest ecosystems are under increasing pressure as a result of climate change, in particular in central Europe, where they are exposed to increasing stress posed by heat and droughts (Thiele et al., 2017). Even more so, an improvement of both the quality and the quantity of EU forests is therefore fundamental to increase their resilience as well as that of urban areas.

4.1. Limitations and uncertainties

The study area encompasses across a multitude of cities characterized by a degree of heterogeneity within and between them. Therefore, the model has been designated in order to be simple and easily scalable/applicable through a wide spatial area. In order to do so, a linear regression model with two predictors has been evaluated as the most appropriate in a cost/benefit perspective. Before selecting these predictors, other additional variables have been tested, such as elevation, imperviousness, distance from sea and water bodies, soil and land cover types, moisture index, density of buildings, and NDVI. Also, other machine-learning algorithms such as random forests and decision trees have been explored. Nevertheless, increasing the complexity of the model with more predictors or with machine learning approaches has not proven to increase in parallel the accuracy and the effectiveness of the model, while on the other hand incurring in autocorrelation or lack of statistical significance problems. Furthermore, it must be noted that the present methodological approach involves potential limitations such as the use of modeled datasets that already entail their own uncertainty and error. In fact, the modeling accuracy is dependent on the inherent complexity of the physical and ecological processes studied, where often multiple interrelations between variables exist. In particular, the PML_V2 transpiration data is derived from a model involving the use of vegetation indices such as Leaf Area Index and climate forcings, including air temperature, as well as its own uncertainty related to data, parametrization and algorithm development (Zhang et al., 2019). In this regard, it could be helpful to include these uncertainties in the calculation of the propagation of the error in future studies

As regards the temporal resolution, the year 2018 has been chosen due to the lack of high-quality data in other years: an additional estimation on a longer period of time has been made (from 2014 to 2017),

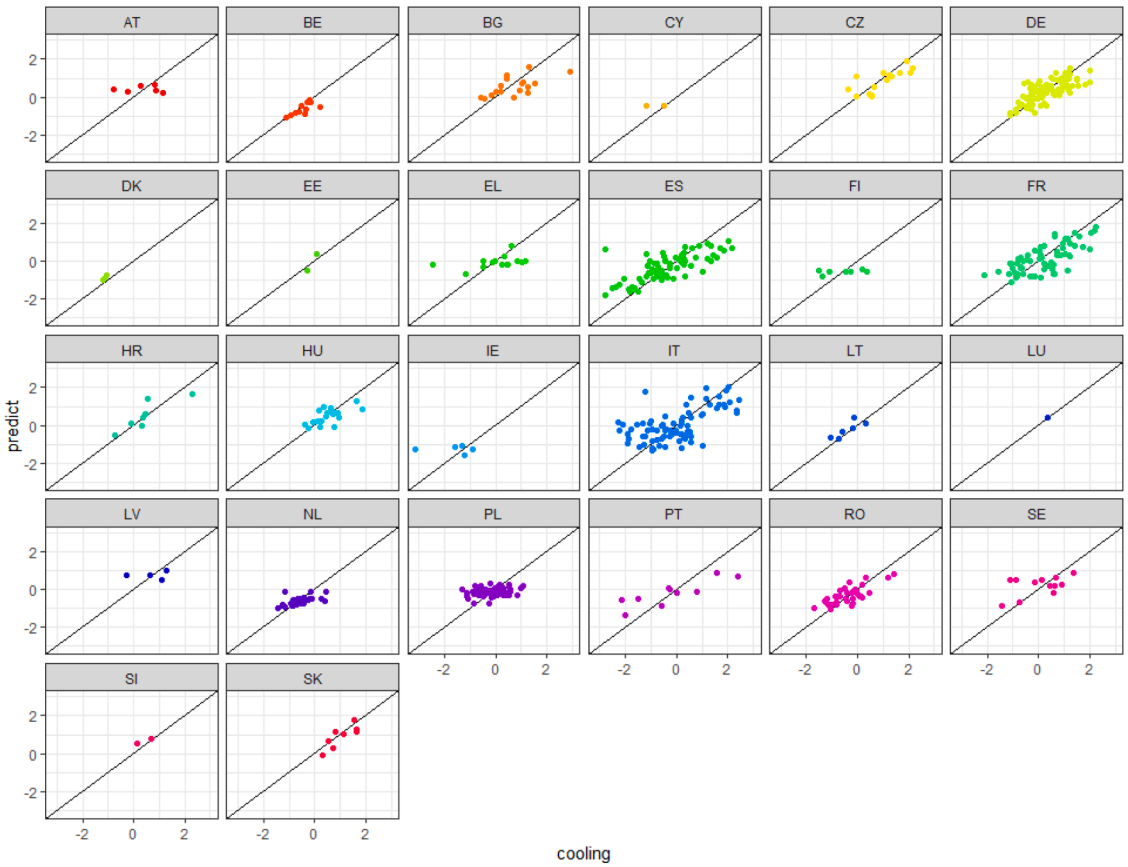

Fig. A.3. Cooling average estimation for the 601 European FUA, paneled by country computed with the multiple regression model M6.

but since it was not possible to retrieve equally reliable data due to the lack of uniform weather conditions across all Europe, the year 2018 has been selected, due to the most reliable land surface temperature data. Furthermore, it has been analyzed also on the basis of its representativeness among other recent years, in terms of temperature anomalies/precipitation.

Finally, it has to be noted that CI value has been estimated in the specific setting of our study and may vary according to different spatio-temporal contexts and spatial scales as well.

5. Conclusion

In this study, a picture of the UHI phenomena in Europe has been provided, investigating the role of Green Infrastructure in mitigating summer urban temperatures in 601 Functional Urban Areas. This approach has shown that trees significantly reduce UHI, with an impact that is dependent by the extent of green areas and amount of transpiration inside a city. In particular, it has been observed that a tree cover of at least 16% is required in order to achieve a reduction of average summer temperature equal to 1 °C. Stakeholders and city administrators can take advantage of the cooling indicator in order to better foresee temperature mitigation strategies in cities, in the view of a sustainable and effective planning. Currently, a significant proportion of urban population does not benefit from the ecosystem service of microclimate regulation, thus being particularly exposed by the detrimental effect of UHI, as well as other unsustainable environmental conditions that often characterize urban areas. Prioritized and targeted interventions on UGI must be aimed to reduce the ecosystem service mismatch, especially in those urban areas located in arid/southern regions and where the amount of tree cover is insufficient. Besides, almost one third (~32%) of European FUAs has a tree cover below 16%. Ecosystems are fundamental allies in the view of a resilient climate adaptation strategy in urban areas, and a rapid implementation of Green Infrastructure is currently a compelling strategy in order to guarantee a sustainable living condition and well-being for urban dwellers.

Declaration of Competing Interest

The Authors declare that there is no conflict of interest.

Appendix A

For the set of 601 cities included in the analysis presented in this paper, the relationship between the estimated value for cooling and a series of variables characteristic of each FUA was analyzed. The explanatory variables considered (at the FUA level) were: total amount of tree cover (% of the FUA), total E_{tree} (mm day^{-1}), elevation (m), population (number of inhabitants), city size (km^2), population density (inhabitant per km^2), city structure (dimensionless) and distance from the sea (m). The models were fitted using the lm() function of the R 4.0.3 base (R Core Team, 2020) and the lmer() function of the nlme4 package (Bates et al., 2014). Several models have been analyzed, in order to estimate if the data contains global and group-level trends, specifically significant differences between the FUA of different countries, as well as to compare the explanatory capacity of the different variables. The proposed regression models were:

- M0: null model. The baseline of comparison is the null hypothesis, where all the regression parameters are equal to 0.
- M1: multiple regression model considering all the aforementioned explanatory variables.
- M2: multiple regression model in which the only explanatory variable is the total amount of tree cover.

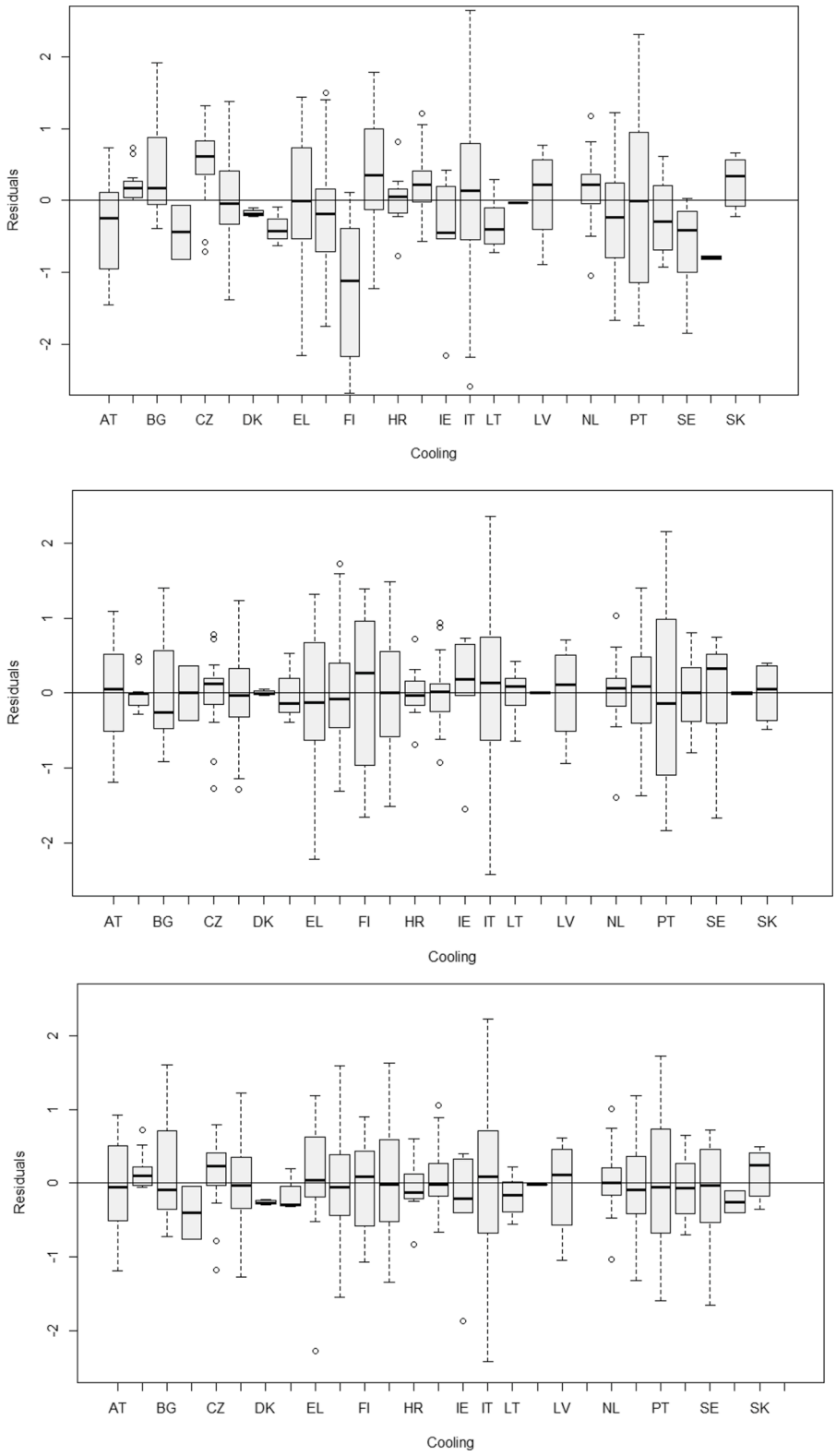

Fig. A.4. Residue distribution by country for the linear regression model M1 (top), the linear fixed effect model M4 (center) and the linear mixed effect M6 (bottom).

- M3: multiple regression model with all explanatory variables of model M1 except for the total amount of tree cover.
- M4: multiple regression model with all explanatory variables from model M1, adding country-specific fixed effects.
- M5: Linear mixed effect models with the country as a factor, with the same explanatory variables as M2.
- M6: Linear mixed effect models with the country as a factor, with the same explanatory variables as M1.

All models show a slight trend of negative residuals for low cooling scores, and positive residuals for high cooling scores. However, this trend is reduced in the models that include the differentiation of FUA

Table A.1
Linear Regression models performance comparison according to different metrics. All models have been created with the dataset of 601 European FUA. The cooling is the response variable for all models. RMSE: Root Mean Square Error (°C); AIC: Aikake Information Criterion.

Model	RMSE	Log-likelihood	AIC
Null Model (M0)	0.9979	−848.7	1701.4
Classical regression (M1)	0.7695	−693.1	1406.1
Classical regression (M2)	0.8233	−733.5	1473.0
Classical regression (M3)	0.8383	−744.3	1506.5
Linear Fixed effect (M4)	0.6999	−636.2	1342.5
Linear Mixed-effects (M5)	0.7429	−705.6	1419.3
Linear Mixed-effects (M6)	0.6780	−658.7	1343.4

Table A.2
Overall performance of the first linear regression of the microclimate regulation model. Determinant coefficient (R2), Root Mean Square Error (RMSE) and Scatter Index (SI) are displayed.

R2	RMSE	SI%
0.44	2.91	9.42

Table A.3
Statistical distribution of Equation's 1 coefficients.

β_{0e1}	β_{1e1}	β_{2e1}
35.89 ± 4.89	−0.07 ± 0.022	−0.01 ± 0.008

Table A.4
Statistical distribution of Equation's 2 coefficients.

β_{0e2}	β_{1e2}	β_{2e2}
40.63±0.44	0.26 ± 0.006	−0.52 ± 0.008

country membership (Fig. A.3). This confirms that there is an influence of country on cooling, especially in some countries such as FI, AT, PT, SE (see Figs. A.1 and A.2). According to the ANOVA analysis, the estimated variability, in the fixed effect model (M4), due to FUA country membership is about 10%. In the mixed effect models (M5 or M6), the estimated variability due to FUA country membership is about 22% of the variance that's left after the variance explained by the fixed effects. The estimated variability due to FUA country membership is about 22% of the total according to models M5 and M6. Table A.1 shows a comparison of the performance of the different models and shows that the best alternatives seem to be the M4 and the M6.

References

R Core Team (2020). R: A language and environment for Statistical Computing. Vienna, Austria: R Foundation for Statistical Computing. Retrieved from http://www.R-project.org/

Bates D, Maechler M, Bolker B, Walker S (2014). lme4: Linear Mixed-Effects Models Using Eigen and S4. R package version 1.1–7, Retrieved from http://CRAN.R-project.org/package=lme4.

Mazerolle MJ (2020). AICcmodavg: Model selection and multimodel inference based on (Q)AIC(c). R package version 2.3–1. Retrieved from https://cran.r-project.org/package=AICcmodavg.

References

Alonso, M. S., Labajo, J. L., & Fidalgo, M. R. (2003). Characteristics of the urban heat island in the city of Salamanca, Spain. *Atmósfera, 16*(3), 137–148.

Zulian, G., Ronchi, S., La Notte, A., Vallecillo, S., & Maes, J. (2021). Adopting a cross-scale approach for thedeployment of a green infrastructure. *One Ecosystem, 6*, e65578. https://doi.org/10.3897/oneeco.6.e65578

Zulian, G., Raynal, J., Hauser, R., & Maes, J. (2021). Urban Green Infrastructure: Opportunities and Challenges at the European scale. In A. Arcidiacono, & S. Ronchi (Eds.), *Ecosystem Services and Green Infrastructure: Perspectives from Spatial Planning in Italy*. Springer International Publishing. https://doi.org/10.1007/978-3-030-54345-7_2.

Bartesaghi-Koc, C., Osmond, P., & Peters, A. (2018). Evaluating the cooling effects of green infrastructure: A systematic review of methods, indicators and data sources. *Solar Energy, 166*, 486–508.

Bokaie, M., Zarkesh, M. K., Arasteh, P. D., & Hosseini, A. (2016). Assessment of urban heat island based on the relationship between land surface temperature and land use/land cover in Tehran. *Sustainable Cities and Society, 23*, 94–104.

Chrysoulakis, N., Grimmond, S., Feigenwinter, C., Lindberg, F., Gastellu-Etchegorry, J. P., Marconcini, M., et al. (2018). Urban energy exchanges monitoring from space. *Scientific Reports, 8*(1), 1–8.

Clinton, N., & Gong, P. (2013). MODIS detected surface urban heat islands and sinks: Global locations and controls. *Remote Sensing of Environment, 134*, 294–304.

Dijkstra, L., & Poelman, H. (2012). Cities in Europe, the new OECD-EC definition. Brussels.

European Commission, (2013). Green infrastructure (GI) – enhancing Europe's natural capital. COM (2013), 249. http://eur-lex.europa.eu/resource.html?uri=cellar:D41348f2-01d5-4abe-b817-4c73e6f1b2df.0014.03/DOC_1&format=PDF.

European Commission, (2019). Review of progress on implementation of the EU green infrastructure strategy. COM (2019), 236 final. 10.1017/CBO9781107415324.004. https://eur-lex.europa.eu/legal-content/EN/TXT/PDF/?uri=CELEX:52019SC0184&rid=9.

European Commission, (2020). EU biodiversity strategy for 2030: Bringing nature back into our lives. COM (2020) 380 Final https://eur-lex.europa.eu/legal-content/EN/TXT/?uri=CELEX:52020DC0380.

European Commission. (2021). *Evaluating the impact of nature-based solutions; a handbook for practitioners*. Luxembourg: Publication office of the European Union.

European Environment Agency. (2020). *Healthy environment, healthy lives: How the environment influences health and well-being in europe*. Luxembourg: Publications Office of the European Union. EEA Report No 21/2019.

Eurostat, Urban Audit, (2020). https://ec.europa.eu/eurostat/web/gisco/geodata/reference-data/administrative-units-statistical-units/urban-audit.

EuroStat, (2016). Urban Europe. https://ec.europa.eu/eurostat/web/products-statistical-books/-/ks-01-16-691.

Eurostat. (2017). *Methodological manual on city statistics –2017 edition*. Luxembourg: Publications Office of the European Union, 2017.

Fischer, E. M., & Schär, C. (2010). Consistent geographical patterns of changes in high-impact European heatwaves. *Nature Geoscience, 3*, 398–403.

Founda, D., & Santamouris, M. (2017). Synergies between urban heat island and heat waves in Athens (Greece), during an extremely hot summer. *Scientific Reports, 7*(1), 1–11.

Freire, S., MacManus, K., Pesaresi, M., Doxsey-Whitfield, E., & Mills, J. (2016). Development of new open and free multi-temporal global population grids at 250 m resolution. *Geospatial data in a changing world*. Association of Geographic Information Laboratories in Europe (AGILE). AGILE, 2016.

Frost, J. (2017). Confidence intervals vs prediction intervals vs tolerance intervals. Statistics by Jim. Retrieved from http://statisticsbyjim.com/hypothesis-testing/confidence-prediction-tolerance-intervals/ Accessed September 9, 2020.

Fusaro, L., Salvatori, E., Mereu, S., Marando, F., Scassellati, E., Abbate, G., et al. (2015). Urban and peri-urban forests in the metropolitan area of Rome: Ecophysiological response of Quercus ilex L. in two green infrastructures in an ecosystem services perspective. *Urban Forestry and Urban Greening, 14*(4), 1147–1156.

Gan, R., Zhang, Y., Shi, H., Yang, Y., Eamus, D., Cheng, L., et al. (2018). Use of satellite leaf area index estimating evapotranspiration and gross assimilation for Australian ecosystems. *Ecohydrology*, e1974. https://doi.org/10.1002/eco.1974

Gong, P., Li, X., Wang, J., Bai, Y., Chen, B., Hu, T., et al. (2020). Annual maps of global artificial impervious area (GAIA) between 1985 and 2018. *Remote Sensing of Environment, 236*, Article 111510.

Haines-Young, R., & Potschin, M. (2018). Common international classification of ecosystem services (CICES) V 5.1. Guidance on the Application of the Revised Structure https://cices.eu/content/uploads/sites/8/2018/01/Guidance-V51-01012018.pdf.

Heris, M., Bagstad, K. J., Rhodes, C., Troy, A., Middel, A., Hopkins, K. G., & Matuszak, J. (2021). Piloting urban ecosystem accounting for the United States. *Ecosystem Services, 48*, 101226.

Jansson, C. E. J. P., Jansson, P. E., & Gustafsson, D. (2007). Near surface climate in an urban vegetated park and its surroundings. *Theoretical and Applied Climatology, 89*(3), 185–193.

Karnieli, A., Ohana-Levi, N., Silver, M., Paz-Kagan, T., Panov, N., Varghese, D., & Provenzale, A. (2019). Spatial and Seasonal Patterns in Vegetation Growth-Limiting Factors over Europe. *Remote Sensing, 11*(20), 2406.

Koppe, C., Kovats, S., Jendritzky, G., Menne, B., Breuer, D., Energy, E., & Deutscher Wetterdienst, S. D. (2004). London school of hygiene and tropical medicine, European commission. *Heat waves: Risks and responses. Regional office for Europe*. Copenhagen: World Health Organization.

Lhotka, O., Kyselý, J., & Farda, A. (2018). Climate change scenarios of heat waves in central Europe and their uncertainties. *Theoretical and Applied Climatology, 131*(3–4), 1043–1054.

Li, Y., Sun, Y., Li, J., & Gao, C. (2020). Socioeconomic drivers of urban heat island effect: Empirical evidence from major Chinese cities. *Sustainable Cities and Society, 63*, Article 102425.

Maes, J., Burkhard, B., & Geneletti, D. (2018). Ecosystem services are inclusive and deliver multiple values. A comment on the concept of nature's contributions to people. *One Ecosystem, 3*, Article e24720.

Maes, J., Zulian, G., Thijssen, M., Castell, C., Baró, F., Ferreira, A. M., … Geneletti, D. (2016). *Mapping and Assessment of Ecosystems and their Services: Urban ecosystems* (p. 4). Luxembourg: Publications office of the European Union.

Manes, F., Marando, F., Capotorti, G., Blasi, C., Salvatori, E., Fusaro, L., & Munafò, M. (2016). Regulating ecosystem services of forests in ten Italian metropolitan cities: air quality improvement by PM10 and O3 removal. *Ecological indicators, 67*, 425–440.

Manoli, G., Fatichi, S., Bou-Zeid, E., & Katul, G. G. (2020). Seasonal hysteresis of surface urban heat islands. *Proceedings of the National Academy of Sciences, 117*(13), 7082–7089.

Marando, F., Salvatori, E., Sebastiani, A., Fusaro, L., & Manes, F. (2019). Regulating ecosystem services and green infrastructure: assessment of urban heat island effect mitigation in the municipality of Rome, Italy. *Ecological Modelling, 392*, 92–102.

Memon, R. A., Leung, D. Y., & Liu, C. H. (2009). An investigation of urban heat island intensity (UHII) as an indicator of urban heating. *Atmospheric Research, 94*(3), 491–500.

Mentaschi, L., Duveiller, G., Zulian, G., Corbane, C., Pesaresi, M., Maes, J. et al. (2021). Global long-term mapping of surface temperature shows intensified intra-city urban heat island extremes.

Mishra, V., Ganguly, A. R., Nijssen, B., & Lettenmaier, D. P. (2015). Changes in observed climate extremes in global urban areas. *Environmental Research Letters, 10*(2), Article 024005.

Morabito, M., Crisci, A., Gioli, B., Gualtieri, G., Toscano, P., Di Stefano, V., et al. (2015). Urban-hazard risk analysis: Mapping of heat-related risks in the elderly in major Italian cities. *PloS One, 10*(5), Article e0127277.

Nouri, H., Borujeni, S. C., & Hoekstra, A. Y. (2019). The blue water footprint of urban green spaces: An example for Adelaide, Australia. *Landscape and Urban Planning, 190*, Article 103613.

Oke, T. R. (1987). *Boundary layer climates* (p. 435). London. New York: Methuen.

Oke, T. R., Mills, G., Christen, A., & Voogt, J. A. (2017). *Urban climates*. Cambridge University Press.

Oke, T. R. (1982). The energetic basis of the urban heat island. *Quarterly Journal of the Royal Meteorological Society, 108*, 1–24. https://doi.org/10.1002/qj.49710845502

O'Malley, C., Piroozfar, P., Farr, E. R., & Pomponi, F. (2015). Urban heat island (UHI) mitigating strategies: A case-based comparative analysis. *Sustainable Cities and Society, 19*, 222–235.

Ottlé, C.&, & Vidal-Madjar, D. (1992). Estimation of land surface temperature with NOAA9 data. *Remote Sensing of Environment, 40*, 27–41.

Parastatidis, D., Mitraka, Z., Chrysoulakis, N., & Abrams, M. (2017). Online global land surface temperature estimation from Landsat. *Remote sensing, 9*(12), 1208.

Potchter, O., Cohen, P., & Bitan, A. (2006). Climatic behavior of various urban parks during hot and humid summer in the Mediterranean city of Tel Aviv, Israel. *International Journal of Climatology: A Journal of the Royal Meteorological Society, 26*(12), 1695–1711.

Qiu, G. Y., Zou, Z., Li, X., Li, H., Guo, Q., Yan, C., et al. (2017). Experimental studies on the effects of green space and evapotranspiration on urban heat island in a subtropical megacity in China. *Habitat international, 68*, 30–42.

Rahman, M.A., Armson, D., & Ennos, A.R. (.2015). A comparison of the growth and cooling effectiveness of five commonly planted urban tree species Urban Ecosystems 18, pp. 371–389.

Saaroni, H., Amorim, J. H., Hiemstra, J. A., & Pearlmutter, D. (2018). Urban green infrastructure as a tool for urban heat mitigation: Survey of research methodologies and findings across different climatic regions. *Urban Climate, 24*, 94–110.

Saaroni, H., Pearlmutter, D., & Hatuka, T. (2015). Human-biometeorological conditions and thermal perception in a Mediterranean coastal park. *International Journal of Biometeorology, 59*(10), 1347–1362.

Schiavina, M., Freire, S., & MacManus, K. (2019). GHS population grid multitemporal ((1975), 1990, 2000, 2015) R2019A. *European Commission, Joint Research Centre (JRC)*. https://doi.org/10.2905/42E8BE89-54FF-464E-BE7B-BF9E64DA5218. PID: Http://data.europa.eu/89h/0c6b9751-a71f-4062-830b-43c9f432370fConcept & Methodology.

Schwarz, N., Schlink, U., Franck, U., & Großmann, K. (2012). Relationship of land surface and air temperatures and its implications for quantifying urban heat island indicators—an application for the city of Leipzig (Germany). *Ecological Indicators, 18*, 693–704.

Sebastiani, A., Marando, F., & Manes, F. (2021). Mismatch of regulating ecosystem services for sustainable urban planning: PM10 removal and urban heat island effect mitigation in the municipality of Rome (Italy). *Urban Forestry and Urban Greening, 57*, Article 126938.

Shashua-Bar, L., & Hoffman, M. E. (2000). Vegetation as a climatic component in the design of an urban street. An empirical model for predicting the cooling effect of urban green areas with trees. *Energy and Buildings, 31*, 221–235.

Singh, P., Kikon, N., & Verma, P. (2017). Impact of land use change and urbanization on urban heat island in Lucknow city, Central India. A remote sensing based estimate. *Sustainable Cities and Society, 32*, 100–114.

Sobrino, J. A., Oltra-Carrió, R., Sòria, G., Jiménez-Muñoz, J. C., Franch, B., Hidalgo, V., et al. (2013). Evaluation of the surface urban heat island effect in the city of Madrid by thermal remote sensing. *International Journal of Remote Sensing, 34*(9–10), 3177–3192.

Somarakis, G., Stagakis, S., & Chrysoulakis, N. (2019).(Eds.)., Thinknature nature-based solutions handbook (10.26225/jerv-w202).

Taylor, J. R. (1997). *An introduction to error analysis: The study of uncertainties in physical measurements*. Sausalito, CA: University Science Books.

Thiele, J. C., Nuske, R. S., Ahrends, B., Panferov, O., Albert, M., Staupendahl, K., et al. (2017). Climate change impact assessment—a simulation experiment with Norway spruce for a forest district in Central Europe. *Ecological Modeling, 346*, 30–47.

Tiwari, A., Kumar, P., Kalaiarasan, G., & Ottosen, T. B. (2021). The impacts of existing and hypothetical green infrastructure scenarios on urban heat island formation. *Environmental Pollution, 274*, Article 115898.

Tsiros, I. X. (2010). Assessment and energy implications of street air temperature cooling by shade trees in Athens (Greece) under extremely hot weather conditions. *Renewable Energy, 35*(8), 1866–1869.

Venter, Z. S., Krog, N. H., & Barton, D. N. (2020). Linking green infrastructure to urban heat and human health risk mitigation in Oslo, Norway. *Science of the Total Environment, 709*, Article 136193.

Von Der Leyen, U. (2019). A union that strives for more my agenda for Europe, political guide-lines for the next European Commission 2019–2024, p 24. Available at: Https://ec.europa.eu/commission/sites/beta-political/files/political-guidelines-next-commission_en.pdf.

Wang, Y., & Akbari, H. (2016a). The effects of street tree planting on urban heat island mitigation in Montreal. *Sustainable Cities and Society, 27*, 122–128.

Wang, Y., & Akbari, H. (2016b). Analysis of urban heat island phenomenon and mitigation solutions evaluation for Montreal. *Sustainable Cities and Society, 26*, 438–446.

Yoshida, A., Hisabayashi, T., Kashihara, K., Kinoshita, S., & Hashida, S. (2015). Evaluation of effect of tree canopy on thermal environment, thermal sensation, and mental state. *Urban Climate, 14*, 240–250.

Yu, Z., Guo, X., Jørgensen, G., & Vejre, H. (2017). How can urban green spaces be planned for climate adaptation in subtropical cities? *Ecological Indicators, 82*, 152–162.

Zhang, X., Estoque, R. C., & Murayama, Y. (2017). An urban heat island study in Nanchang City, China based on land surface temperature and social-ecological variables. *Sustainable Cities and Society, 32*, 557–568.

Zhang, Y., Kong, D., Gan, R., Chiew, F. H. S., McVicar, T. R., Zhang, Q., et al. (2019). Coupled estimation of 500 m and 8-day resolution global evapotranspiration and gross primary production in 2002–2017. *Remote Sensing of Environment, 222*, 165–182. https://doi.org/10.1016/j.rse.2018.12.031

Zhou, B., Rybski, D., & Kropp, J. P. (2017). The role of city size and urban form in the surface urban heat island. *Scientific Reports, 7*(1), 1–9.

Zulian, G., Thijssen, M., Günther, S., & Maes, J., 2018. Enhancing Resilience Of Urban Ecosystems through Green Infrastructure (EnRoute).

Maes, J., Zulian, G., Günther, S., Thijssen, M., & Raynal, J., 2019. Enhancing resilience of urban ecosystems through green infrastructure (EnRoute). Inception Report.